Received: 17 December 2016 | Revised: 12 September 2017 | Accepted: 21 September 2017

DOI: 10.1111/pce.13085

WILEY Plant, Cell & Environment

ORIGINAL ARTICLE

Gene expression trade-offs between defence and growth in English elm induced by *Ophiostoma novo-ulmi*

Pedro Perdiguero[1,2] | Juan Sobrino-Plata[1] | Martin Venturas[1,3] | Juan Antonio Martín[1] | Luis Gil[1] | Carmen Collada[1]

[1] GENFOR, Grupo de Investigación en Genética, Fisiología e Historia Forestal, Universidad Politécnica de Madrid (UPM), 28040 Madrid, Spain

[2] iBET, Instituto de Biologia Experimental e Tecnológica, Apartado 12, 2781-901 Oeiras, Portugal

[3] Biology Department, University of Utah, Salt Lake City, UT 84112, USA

Correspondence
Carmen Collada, GENFOR, Grupo de Investigación en Genética y Fisiología Forestal, Universidad Politécnica de Madrid, Ciudad Universitaria s/n, E-28040 Madrid, Spain.
Email: carmen.collada@upm.es

Funding information
People Programme (Marie Curie Actions) of the European Union's Seventh Framework Programme, Grant/Award Number: FP7/2007-2013; Spanish National Research Plan, Grant/Award Number: AGL2015-66925-R MINECO/FEDER, UE AGL2012-35580; Ministerio de Agricultura, Alimentación y Medio Ambiente (MAGRAMA)

Abstract

Wilt diseases caused by vascular pathogens include some of the most damaging stresses affecting trees. Dutch elm disease (DED), caused by the fungus *Ophiostoma novo-ulmi*, destroyed most of North American and European elm populations in the 20th century. The highly susceptible English elm, also known as Atinian clone, suffered the highest mortality rates during the last pandemic event, probably due to its lack of genetic diversity. To study the DED pathosystem, we inoculated English elm ramets with *O. novo-ulmi* and evaluated xylem anatomy, molecular response, and disease symptoms. The high DED susceptibility of the clone was linked to xylem structure. The transcript levels changed significantly for 1,696 genes during *O. novo-ulmi* invasion. Genes covering different steps of the plant immune system were identified, many of which showed homology with *Arabidopsis thaliana* genes involved in systemic acquired resistance. Induction of several pathogenesis-related proteins and repression of fasciclin-like arabinogalactan proteins and other cell wall biosynthesis pathways evidence unbalanced costs between growth and defence mechanisms far from the inoculation point. This study sheds light on elm molecular defence mechanisms against DED.

KEYWORDS

Dutch elm disease, microarrays, plant immune system, systemic acquired resistance, *Ulmus minor*, vascular pathogen

1 | INTRODUCTION

Trees are exposed to many instances of environmental interaction and stress throughout their life cycle. These include pests and diseases that can cause dramatic mortality events in forests and loss of foundation species and iconic trees (e.g., Ellison et al., 2005). Diseases affecting tree vascular systems are usually very harmful due to the crucial role of these tissues in transporting water, nutrients, hormones, and other compounds. Dutch elm disease (DED) is a vascular wilt disease caused by the pathogenic fungi *Ophiostoma ulmi* (Buisman) Melin & Nannf and the more virulent *Ophiostoma novo-ulmi* (Brasier; Brasier, 2000). Spores of DED fungi are transmitted from infected to healthy trees by elm bark beetles (*Scolytus* spp. and *Hylurgopinus* spp.) during feeding on twig phloem (Anderbrant, Yuvaraj, Martin, Gil, & Witzell, 2017; Faccoli & Battisti, 1997). Once spores have germinated in the feeding groove, hyphae spread within xylem vessels and induce blockage and cavitation, resulting in foliar wilting and eventually tree death (Li et al., 2016; Venturas, López, Martín, Gascó, & Gil, 2014). Two DED pandemics last century severely damaged North American and European elm populations (Brasier, 2000). Field elm (*Ulmus minor* Mill.) was the species most affected by DED in Europe, where the disease killed more than 25 million trees in Britain alone and decimated 80–90 % of this species in Spain (Domínguez Lerena, 2002).

The rapid spread of DED across Europe was probably favoured by large-scale human-induced reduction of field elm genetic diversity (Martín, Fuentes-Utrilla, & Witzel, 2010). English elm (*Ulmus procera* Salisb.) was shown to be a single *U. minor* clone of Italian origin known as Atinian elm, massively propagated during the Roman Empire to support and train grapevines (Gil, Fuentes-Utrilla, Soto, Cervera, & Collada, 2004). The Atinian elm was introduced in all countries where the Romans established viticulture (Spain, Portugal, Switzerland, Germany, and England), affecting the genetic diversity of natural elm populations due to the high capacity of this elm for asexual propagation from root suckers and cuttings and its inability to set seeds. The resulting genetic homogeneity of elm stands and the high susceptibility of this clone to

DED may have favoured the spread of the disease during pandemic events (Gil et al., 2004).

Despite the major impact of DED pandemics on Atinian elms, some iconic ornamental trees surviving in cities and villages and other individuals in seminatural elm populations such as Rivas-Vaciamadrid (Madrid, Spain) belong to this clone (Gil et al., 2004; Martín, Solla, Burón, López-Almansa, & Gil, 2006). Atinian elms commonly occur as immature trees in most European countries affected by DED due to the ability of the clone to resprout from roots (Dunn, 2000). The prevalence of this susceptible clone and its role in the spread of DED pandemics make it particularly suitable for advancing knowledge of how *O. novo-ulmi* interacts with *U. minor* during vascular colonization.

Diseases affecting plant vascular systems, known as wilt diseases, cause severe damage and are difficult to study because of their complexity (Yadeta & Thomma, 2013). As Bernier et al. (2015) reported, the pathosystem formed by interaction between *Ulmus* spp. and *O. ulmi* or *O. novo-ulmi* has often been analysed in a very reductionist manner. The limited molecular knowledge of the DED pathosystem contrasts with current knowledge of plant–pathogen interactions in model plants. Research on these organisms has elucidated the molecular bases of these interactions. Plants have developed various molecular pathways integrated into a complex plant immune system. Plant cells sense invading pathogens via extracellular receptors known as pattern recognition receptors. This innate immune system identifies general or specific conserved microbe-specific molecules, referred to as microbe- or pathogen-associated molecular patterns (MAMPs or PAMPs), which induce a first cascade of defence called MAMP- or PAMP-triggered immunity (MTI or PTI) (Jones & Dangl, 2006).

A second line of plant defence is activated after direct or indirect recognition of a given effector by a set of plant resistance (R) gene products, resulting in effector-triggered immunity (ETI; Jones & Dangl, 2006). R proteins are commonly intracellular receptors containing leucine-rich repeats (LRRs), although other R genes without this domain have been described (Gururani et al., 2012). Once plant cell receptors sense a pathogen, both MTI/PTI and ETI are activated to coordinate the plant defence response, essentially as correlative phenomena. The major signalling pathways involved in posterior signal transduction in response to pathogens are mediated by kinases, reactive oxygen species (ROS), and proteins modulating signalling driven by concentrations of calcium ions (Ca^{2+}). These cascades modulate the expression of transcription factors (TFs) or genes involved in the synthesis of new regulators, mainly salicylic acid (SA) and jasmonic acid (JA; Moore, Loake, & Spoel, 2011; Pieterse, Leon-Reyes, Van der Ent, & Van Wees, 2009). SA and JA are thought to form the backbone of the plant defence system. Other hormones, such as ethylene, abscisic acid, gibberellins, auxins, and cytokinins, are able to modulate the SA- and JA-dependent signalling pathways (Pieterse, Van der Does, Zamioudis, Leon-Reyes, & Van Wees, 2012). Accumulation of endogenous SA is required to activate systemic acquired resistance (SAR), a long-lasting, broad-spectrum induced resistance characterized by coordinated activation of a specific set of pathogenesis-related (PR) proteins, most of which have antimicrobial activity (Van Loon, Rep, & Pieterse, 2006).

Earlier studies on elm responses to DED focused on individual components produced by the tree, such as phytoalexins (Jeng, Alfenas, Hubbes, & Dumas, 1983), lignin and suberin (Aoun, Rioux, Simard, & Bernier, 2009; Martín, Solla, Woodward, & Gil, 2007), and phenolic compounds (Aoun et al., 2009; Krause, Ichida, Schreiber, & Domir, 1996; Rioux & Ouellette, 1991), or on fungal molecules such as cerato-ulmin (Takai & Hiratsuka, 1984) and peptidorhamnomannans (Nordin & Strobel, 1981). More recently, *in vitro* and *in vivo* studies have started to unravel *Ulmus–Ophiostoma* interaction from a molecular perspective, reporting variation in expression of several defence-related genes encoding enzymes involved in phytoalexin biosynthesis, various PR proteins, and genes associated with the phenylpropanoid pathway (Aoun et al., 2009; Nasmith, Jeng, & Hubbes, 2008; Sherif, Shukla, Murch, Bernier, & Saxena, 2016). New omics technologies have significantly increased the genetic information available for *Ulmus* spp. Resources include recent sequencing of an expressed sequence tag (EST) library in response to elm leaf beetle (*Xanthogaleruca luteola*) infestation and spraying with methyl jasmonates (Büchel et al., 2012) and a first transcriptome in response to abiotic and biotic stresses (Perdiguero, Venturas, Cervera, Gil, & Collada, 2015b). In the latter case, *U. minor* genotypes with contrasting DED tolerance were inoculated with *O. ulmi* and *O. novo-ulmi* and subjected to other stresses.

In this study, we hypothesize that *O. novo-ulmi* is a hemibiotrophic pathogen, which induces JA- and/or SA-mediated signalling pathways in xylem tissues of infected plants. As a result, these induced pathways lead to the overexpression of specific defence responses in distal parts of the plant. As *O. novo-ulmi* is a vascular pathogen, we also hypothesize that the xylem anatomical features of the English elm and the structural defences induced by *O. novo-ulmi* in its vascular tissues are related to the high susceptibility of this clone. To test these hypotheses, 6-year-old Atinian elm ramets were inoculated with *O. novo-ulmi* to evaluate their defence responses. Xylem anatomical structures (where the pathogen spreads) and the long-distance (systemic) molecular responses activated during plant colonization were analysed. To elucidate the genes involved in the *U. minor* immune system and the molecular changes after inoculation, oligomicroarrays were constructed using the data from the transcriptome available in the Dryad database (Perdiguero, Venturas, Cervera, Gil, & Collada, 2015a) and hybridized with cDNA obtained from the ramets over a time course post inoculation. To the best of our knowledge, this is the first study to address the global differential expression of *U. minor* genes during *in vivo* colonization of *O. novo-ulmi*. Numerous genes and pathways showed significant changes, some previously reported in other plant species. The results allow us to advance knowledge of molecular responses that may be specific to vascular wilt diseases and, in particular, of the recognition of genes unique to the DED pathosystem.

2 | MATERIALS AND METHODS

2.1 | Plant material

Twelve ramets from elm genotype VA-AP38 (Arrabal del Portillo, Valladolid) propagated in 2008 from hardwood cuttings were

planted in a research plot at Puerta de Hierro Forest Breeding Centre (Madrid, Spain; 40.456238 N, 3.751823 W) in spring 2009. Ramets were planted 1.0 × 0.75 m apart. The plot was watered during spring and summer to ensure plant establishment and growth and avoid drought stress.

Genotype VA-AP38 was identified as Atinian elm using molecular markers, following the process described by Martín et al. (2015). Leaf DNA was extracted following the protocol of Dumolin, Demesure, and Petit (1995). The chloroplast lineage was analysed with two markers (SFm and ccmp2), and 10 nuclear microsatellites (Ulmi1–98 and Ulmi1–165; Ulm2, Ulm3, and Ulm8; UR 123, UR 141, UR 153, UR 158, and UR 159) were used to determine whether the genotype belonged to the Atinian elm clone. The primer and polymerase chain reaction (PCR) conditions are shown in Table S1.

2.2 | Inoculation, sampling times, and symptom analysis

At the beginning of May 2013, when the ramets were 6 years old, an aggressive local strain of *O. novo-ulmi* (Z-BU1) was inoculated into the selected genotype following the procedure described by Solla, Martín, Ouellette, and Gil (2005). Inoculation was performed about 20 days after full leaf expansion by introducing at midday (during maximum transpiration rates) 0.1 ml of a suspension of *O. novo-ulmi* spores (10^6 spores ml^{-1}) into the sap stream through a wound made at the base of the trunk with a sharp blade. Each experimental unit, randomly distributed in the plot, consisted of two consecutive ramets. One ramet was inoculated with *O. novo-ulmi* spore suspension and the other with distilled water as a control. A healthy 3-year-old branch at approximately 2 m height was collected at 1, 3, 7, 14, and 21 days post inoculation (dpi) from inoculated and control plants at midday. The first branch segment (5 cm) was collected for anatomical structure analysis. Branches were tagged and immediately frozen in liquid nitrogen and stored at −80 °C. Disease development was evaluated in previously selected branches by estimating the percentage of wilting leaves. These observations were performed at sampling times (1, 3, 7, 14, and 21 dpi) and at 28, 60, and 120 dpi.

2.3 | Characterization of anatomical structure

Anatomical parameters were measured in two control ramets. Two additional ramets inoculated with the pathogen were sampled to visualize xylem responses to infection by *O. novo-ulmi*. Four 3-year-old twig segments (3 cm length, 1.3–1.9 cm diameter) were taken from the cardinal points of the crown of each tree and immediately placed in formalin–acetic alcohol (formaldehyde:acetic acid:70% ethanol, 5:5:9 v/v/v) fixative. Samples were taken from control ramets at Day 0 and from inoculated plants at Day 120 post inoculation.

Twig samples were sectioned in radial, transverse, and tangential cuts (20 μm thick) using a Leica SM2400 Sledge Microtome. Cuts were dehydrated through an alcohol series, placed on glass slides, stained with safranine 0.1% (*w/v*), and fixed with Canada balsam. Sections were examined under an Olympus BX50 light microscope connected to a personal computer. Measurements were taken from the 2013 growth increment using ImageJ software (http://rsbweb.nih.gov/ij/).

Bordered pit measurements were made on radial sections using pits located in earlywood vessels with radial diameters of 60–100 μm. Pit membrane diameter and pit aperture area were recorded. All earlywood vessels in the radial section of the 2013 annual ring were included. At least eight sections per sample, comprising 50–60 measurements per ramet, were evaluated.

Earlywood vessel measurements were made on transverse sections, randomly selecting four radial 500-μm-wide sectors 90° apart in the earlywood. Vessel diameters were measured radially in each sector, disregarding vessels less than 20 μm in diameter. The Hagen–Poiseuille equation (Giordano, Salleo, Salleo, & Wanderlingh, 1978) was used to estimate the relative theoretical hydraulic conductance (THC) of vessels by dividing the sum of the fourth power of internal vessel radii by the sector area. Vessel transectional area was obtained by dividing the area occupied by the vessels in a sector by the total area of the sector then multiplying by 100. At least four sections per sample, comprising 100–200 measurements per ramet, were used.

Tangential sections were used to measure ray tangential area (area occupied by the rays in a sector by the total area of the sector, multiplied by 100). At least eight sections per sample, comprising 50–60 measurements per ramet, were examined.

2.4 | Microarray design and hybridization

Encoding a range of proteins, 14,898 isotigs were obtained from a transcriptome described by Perdiguero et al. (2015a) and included in the microarray design (Agilent 8 × 60 K, Agilent Technologies, CA, USA). For each isotig, one 60-base-long probe was designed and spotted at least 3 times on the slide. Probes designed for *Populus*, mouse, and human ESTs available in public databases were included as negative controls.

Total RNA for each sampling time was extracted from branches following the CTAB–LiCl precipitation method (Chang, Puryear, & Cairney, 1993). RNA was purified using the Qiagen RNAeasy kit (Qiagen, CA). RNA amplification and labelling were performed following Adie et al. (2007). Three biological replicates for control and inoculated plants for each sampling time (1, 3, 7, 14, and 21 dpi) were hybridized using two colours (inoculated vs. control). "The manual two-colour microarray-based gene expression analysis" protocol (Agilent Technologies, CA, USA) was followed for hybridizations. Images from Cy3 and Hyper5 channels were equilibrated and captured with a GenePix 4000B (Axon, CA, USA) and spots quantified using the GenePix software (Axon, CA, USA). The microarray design and hybridization data were deposited in ArrayExpress database under accession numbers A-MTAB-611 and E-MTAB-5654, respectively.

2.5 | Data analysis

Background correction and normalization of expression data were performed using Linear Models for Microarray Data (Smyth, 2004; Smyth & Speed, 2003), part of "Bioconductor, an R language project"

(www.bioconductor.org). For local background correction and normalization, the methods "normexp" and "loess" in Linear Models for Microarray Data were used, respectively. To achieve similar distribution across arrays and consistency among arrays, log-ratio values were scaled using the median absolute value as scale estimator. Differentially expressed genes (DEGs) were evaluated by the non-parametric algorithm "Rank Products," available as the "RankProd" package at "Bioconductor, an R language project" (Breitling, Armengaud, Amtmann, & Herzyk, 2004; Hong et al., 2006). This method detects genes that are consistently high ranked in a number of replicated experiments independently of their numerical intensities. Results are provided in the form of *p*, defined as the probability that a given gene is ranked in the observed position by chance. The expected false discovery rate was controlled to be less than 5 %.

Changes in the expression of a gene relative to control plants were estimated using the average signal intensity across the dataset from three biological replicates. Based on the statistical analysis, a gene was considered to be significantly up- or down-regulated for a genotype if it met all three of the following criteria: (a) FDR Rank Prod $p < .05$; (b) fold change ≥1.6 for up-regulation or ≤−1.6 for down-regulation at any sampling time, and (c) the trend (up- or down-regulation) was consistent in all datasets for each isotig. Hierarchical clustering of DEGs was performed using the log2 of average expression value from three biological replicates and K-means method, selecting 12 clusters as threshold of the MeV 4.4 software (Saeed et al., 2006).

2.6 | Single enrichment and gene set enrichment analysis

Full GO (Gene Ontology) term annotation and KEGG (Kyoto Encyclopedia of Genes and Genomes) pathways information from the *U. minor* transcriptome available in Dryad database (Perdiguero et al., 2015a) were used in functional analysis of DEGs.

GO term enrichment was analysed for every trend according to clustering by comparison with the remaining selected significant genes identified during *O. novo-ulmi* invasion, using FatiGO (Al-Shahrour, Díaz-Uriarte, & Dopazo, 2004) implemented in Blast2GO software. This programme conducts a Fisher's exact test for 2 × 2 contingency tables to check for significant over-representation of GO annotations. GO term enrichment was significant at $p < .05$.

KEGG pathway enrichment analysis was performed using GSEA software (Subramanian et al., 2005). Every gene set represents a full KEGG pathway and was defined as the aggrupation of all genes identified along the pathway. A data matrix containing the log2 of average expression value from three biological replicates was used to analyse pathways positively or negatively correlated with the main trend. Time course analysis using Pearson's correlation was applied with a 1,000 gene set permutation. Change in pathways was significant at $p < .05$.

2.7 | Real-time quantitative PCR

Validation of the transcriptome profiling experiment was performed on selected genes identified from the microarray experiment by real-time reverse transcription polymerase chain reactions (RT-PCRs) using RNA from one of the samples used as a biological replicate in the microarrays. For RT-PCR, RNA was treated with DNAse Turbo (Ambion; Applied Biosystems, Life Technologies, CA, USA). First-strand cDNA was synthesized from 1 μg total RNA from each sample using PowerScriptIII reverse transcriptase (Invitrogen) according to the supplier's manual. After verifying that the signal intensity remained unchanged across *Ophiostoma* invasion, 18S rRNA was used as a control.

The primers for the selected genes are shown in Table S2. PCRs were performed in an optical 96-well plate with a CFX 96 detection system (Bio-Rad), using EvaGreen to monitor dsDNA synthesis. Reactions containing 2× SsoFast EvaGreen Supermix reagent (Bio-Rad, CA, USA), 12.5 ng cDNA, and 500 nM of primers in a final volume of 10 μl were subjected to the following standard thermal profile: 95 °C for 3 min, 40 cycles of 95 °C for 10 s, and 60 °C for 10 s. Three technical replicates were performed for each PCR run. To compare the data from different PCR runs or cDNA samples, the mean of the threshold cycle (CT) values of the three technical replicates was normalized to the mean CT value of Ri18S. The expression ratios were then obtained using the ΔΔCT method corrected for the PCR efficiency for each gene (Pfaffl, 2001).

3 | RESULTS

3.1 | Identification of Atinian elm by molecular markers

Chloroplast DNA analysis showed that VA-AP38 belongs to the same Italian linage as the Atinian clone (Table 1), and the alleles found for the 10 nuclear loci tested revealed that VA-AP38 had the same genotype as Atinian clone reference samples from England and Spain (Gil et al., 2004).

3.2 | Symptom analysis

Plants were visually analysed to evaluate symptoms in the 4 months post inoculation. *O. novo-ulmi* inoculated plants showed the first DED symptoms at 14 dpi, when 10–15 % of their leaves were wilted. Wilting values were above 50 % at 21 dpi, the final sampling time for molecular analysis. At later dates (28, 60, and 120 dpi), all *O. novo-ulmi* infected plants showed wilting values above 80 %. No DED symptoms were observed in control plants during the experiment (Figure 1).

3.3 | Anatomical structure

Atinian clone showed wide earlywood vessels and high values of vessel transectional area and THC compared with data reported for twig samples of Siberian elm (*Ulmus pumila*) and *U. minor* clones tolerant to DED (Table 2). The pit membrane diameter of Atinian elm was similar to values found in *U. pumila* and tolerant *U. minor*, but pit aperture area was larger. The tangential section had large medullary rays and therefore a higher proportion of ray parenchyma cells than in *U. pumila* and tolerant *U. minor*. In the ramets inoculated with *O. novo-ulmi*,

TABLE 1 Genetic characterization of VA-AP38

	SFm		ccpm2		Ulmi1–98		Ulmi1–165		Ulm2		Ulm3		Ulm8		UR 123		UR 141		UR 153		UR 158		UR 159	
VA-AP38	297		215		126	151	146	156	102	108	176	176	196	196	250	252	158	160	184	188	179	188	258	278

Note. Alleles for the two chloroplast DNA markers and 10 nuclear microsatellites used are shown.

FIGURE 1 Evaluation of symptoms caused by *Ophiostoma novo-ulmi* infection. An experimental unit of the VA-AP38 genotype of Atinian clone 120 days post inoculation. Left: Control plant in which no symptoms were observed. Right: Inoculated plant showing high degree of wilting. Table under figure shows average percentage of wilting observed in inoculated trees during disease development. Photo: Jorge Domínguez Palacios

abundant tylosis formation was observed in earlywood vessels at 120 dpi (Figure 2).

3.4 | Identification, clustering, and functional analysis of DEGs

Time course analysis revealed that 1,696 of the isotigs included in the microarray (approximately 12 %) showed significant differences in transcription levels during *O. novo-ulmi* infection; these were considered DEGs. DEGs were clustered in 12 main trends by transcription patterns (Figure 3 and Table S3). Most of the DEGs correspond to two profiles: six clusters (C1, C2, C6, C9, C11, and C12; 42.33 % of DEGs) predominantly showed inductions in mean trends, whereas the other six (C3, C4, C5, C7, C8, and C10) mainly presented decreases in transcript levels during *O. novo-ulmi* colonization. C1 included the genes most induced during infection. The transcript levels of these genes increased progressively from the first dpi. A similar trend was observed in C12, although the expression level was lower than C1. In contrast, genes included in C2 showed highest induction during the first 24 hr post inoculation. C6 grouped genes with moderate increases in transcript levels at intermediate sampling times, mainly 3 and 7 dpi. The final clusters showing induction of genes, that is, C9 and C11, included genes with strong increases in transcript levels at 21 dpi, with higher expression values in C11. Clusters with repression in expression patterns, C3, C4, and C5, evidenced a progressive decrease in transcript levels, with lower expression values at 21 dpi. C5 was the cluster that included the most repressed genes. Clusters C7 and C8 grouped genes with decreases in transcript levels at 14 dpi, with C7 maintaining the repression at 21 dpi, whereas C8 recovered similar expression to control plants at 21 dpi. C10 included genes with moderate repression at 3 and 7 dpi.

Single enrichment analysis was performed by comparing functionalities assigned to the 1,696 DEGs and those identified within the 14,898 genes included in the array design. In the class "cellular component," the functional categories "cell wall," "extracellular region," and "plasma membrane" were over-represented in DEGs.

TABLE 2 Mean xylem parameters (and range values) measured in 3-year-old branches of Atinian elm and *Ulmus pumila* and tolerant *Ulmus minor* clones reported in a previous work

Anatomical trait	Atinian elm	*U. pumila*[a]	Tolerant *U. minor*[a]
Earlywood vessel diameter (μm)	55.8 (20.4–125.8)	49.5 (27.0–119.6)	48.5 (27.4–89.4)
VTA (%)	32.9 (17.0–68.0)	25.2 (21.3–30.6)	16.9 (12.4–28.9)
THC (μm^2)	251.9 (93.8–429.1)	129.2 (21.3–30.6)	79.5 (12.4–28.9)
Pit membrane diameter (μm)	7.0 (5.3–9.5)	7.2 (4.8–9.4)	7.2 (4.5–11.3)
Pit aperture area (μm^2)	4.6 (2.9–6.3)	2.4 (0.8–4.8)	2.7 (0.8–5.8)
Ray tangential area (%)	10.1 (6.2–14.7)	7.5 (6.3–9.2)	8.5 (7.4–10.0)

[a]Values reported in Martín et al. (2009).

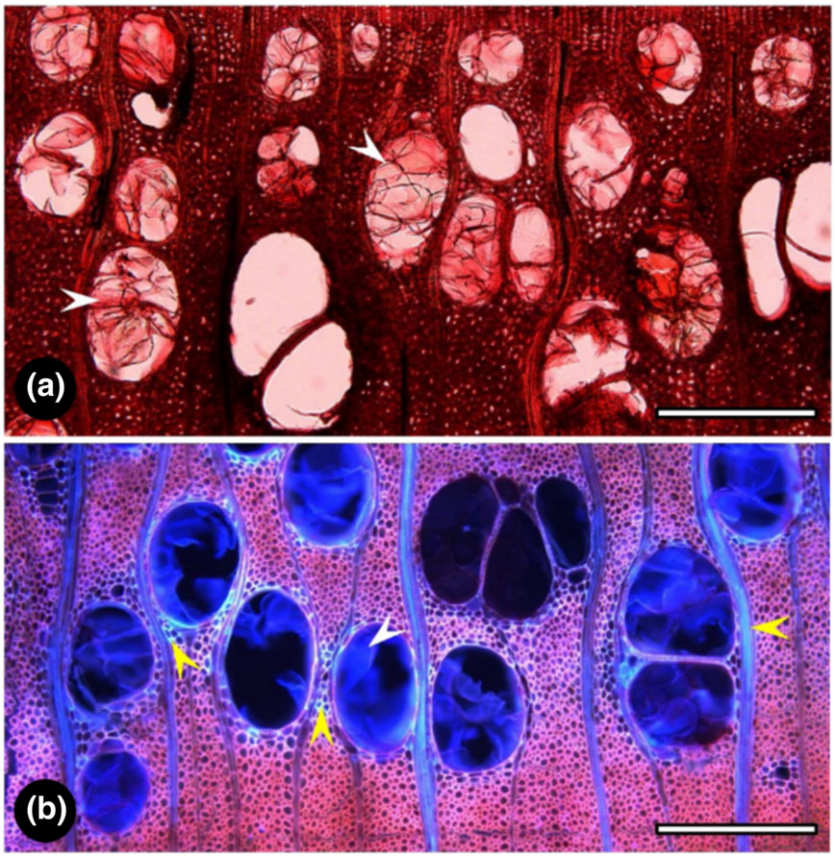

FIGURE 2 Atinian elm micrographs of transverse sections showing responses to *Ophiostoma novo-ulmi*. Sections correspond to twig samples harvested at 120 days post inoculation and observed under (a) tungsten and (b) UV illumination. A high proportion of earlywood vessels were occluded with gels and tyloses (white arrowheads), showing fluorescence under UV illumination. Some paratracheal and ray cells also showed fluorescent reactions (yellow arrowheads), most likely corresponding to suberin presence. Bar = 100 μm

Also, in the class "biological process," all the functional categories related with response ("stress," "abiotic," "biotic," "extracellular," and "endogenous stimulus") and other categories including "secondary metabolic process," "signal transduction," "cell growth," "cell death," or "transport" were significantly enriched within DEGs (Figure S1).

Several GO term categories were associated with trends previously identified in clustering analysis. Global functional analysis of clusters at Level 2 in the class "biological process" (Figure 3) showed that the GO terms "signalling," "response to stimulus," and "biological regulation" are therefore slightly over-represented in clusters showing clear induction during disease development. In contrast, in clusters showing repression throughout infection, GO terms "reproduction," "multicellular organismal process," "growth," and "developmental process" presented higher percentages. Enrichment analysis between clusters, comparing GO terms from biological processes or molecular functions, showed clear enrichment in some functionalities for every cluster (Figure 4). Significant enrichment ($p < .05$) in GO terms "cell death," "response to biotic stimulus," "response to stress," "response to endogenous stimulus," and "response to external stimulus" was found in all clusters with overexpression patterns. Specific functionalities were observed in certain clusters, for example, "oxygen binding," "sequence-specific DNA binding transcription factor activity," and "signal transduction" in C2, "protein binding" in C6, and "transport," "transporter activity," and "transferase activity" in C9. In repressed gene clusters, significant enrichment of GO terms "anatomical structure morphogenesis," "cell growth," and "cell differentiation" was observed in C3 and C4, whereas in C7, C8, and C10, enrichment occurred in GO term "response to abiotic stimulus" and in other terms at a lower percentage.

3.5 | *U. minor* genes involved in response to *O. novo-ulmi*

Genes notably overexpressed or repressed compared to noninoculated plants were identified from the 1,696 DEGs during *O. novo-ulmi* invasion, mainly at 14–21 dpi. The 25 top up-regulated genes were all included in Cluster 1 or 11. These genes reached 50- to 350-fold higher average expression values in infected plants than in controls. Various PR proteins were encoded by 16 of the 25 induced genes. The remaining nine genes encoded five enzymes (valencene synthase, UDP-glycosyltransferase, 2-methylene-furan-3-one reductase, phenylalanine ammonia-lyase, and feruloyl ortho-hydroxylase) and one plant basic secretory family protein, and three genes were annotated as hypothetical or uncharacterized proteins. In contrast, the transcript levels of the 25 top down-regulated genes reached values of −30- to −170-fold in infected relative to control plants (Table 3). The most repressed genes included five encoding fasciclin-like arabinogalactan proteins (FLAs), one encoding the enzyme germacrene D synthase, one encoding an aquaporin, and one encoding a tubulin. Notably, no homology with known proteins was found for eight strongly repressed genes.

In addition to these PR proteins, other well-known genes were identified in the DEGs, including receptors potentially involved in the perception of *O. novo-ulmi*, kinases and other genes involved in signal

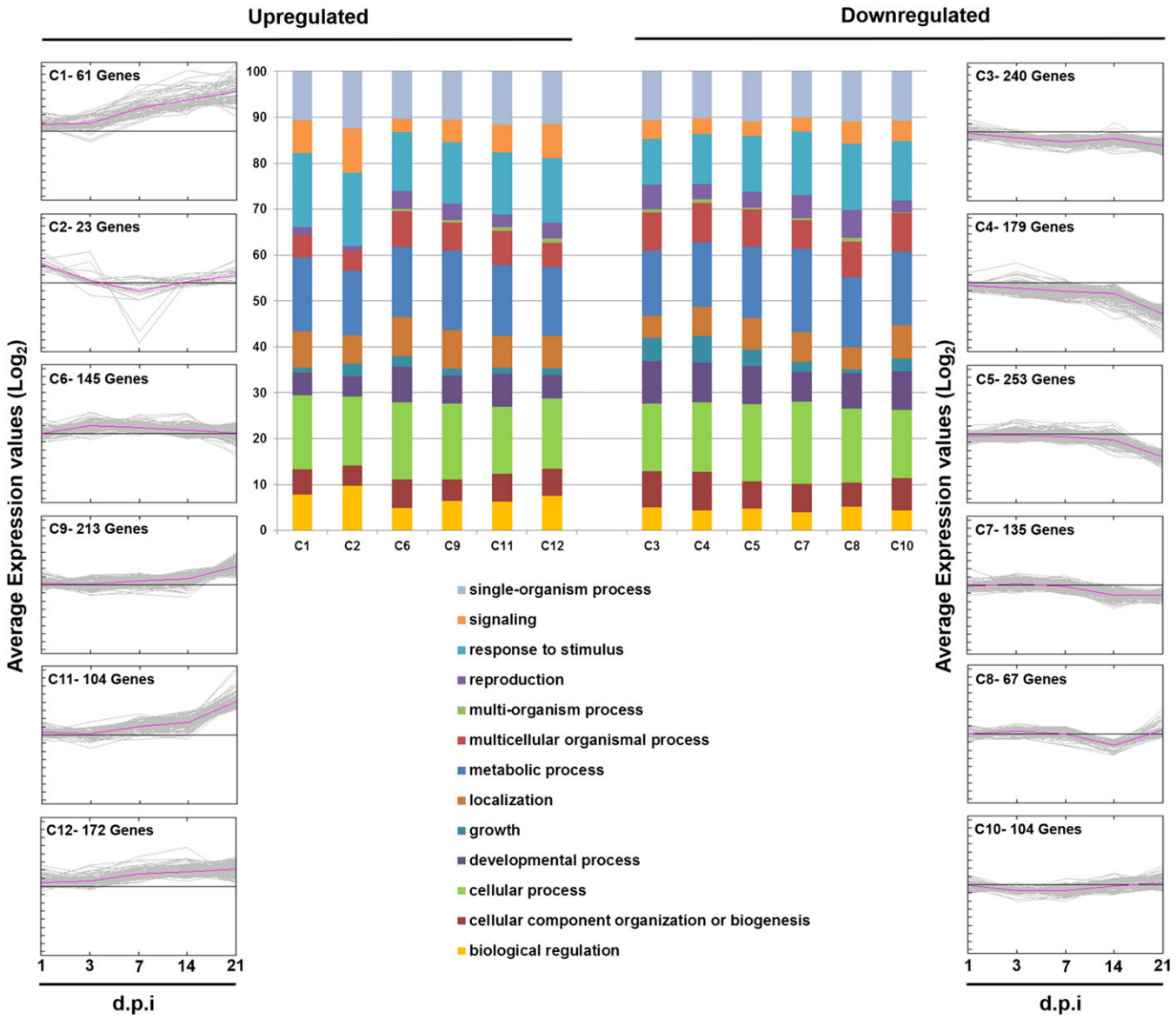

FIGURE 3 Clustering and Gene Ontology (GO) term distribution for each cluster. K-means clustering (k = 12) of differentially expressed genes, representing main tendencies of gene expression profiles during *Ulmus* infection by *Ophiostoma novo-ulmi*. The number of genes included in each cluster is indicated. The internal panel shows the percentage of GO terms identified at Level 2 of GO classification for each cluster relative to total annotations in this level

transduction, and genes encoding TFs potentially involved in activation of defence genes.

3.5.1 | Genes involved in perception

In total, 76 *U. minor* genes, grouped in clusters by expression pattern, were identified as receptors or annotated with GO term "receptor activity" (GO:0004872). Of these, 45 showed increased transcript levels during infection and 31 showed decreased levels (Table S4). At least 39 genes contained an LRR domain. Three *U. minor* genes up-regulated during *O. novo-ulmi* invasion were identified as R protein receptors, nucleotide-binding site-leucine-rich receptor-interleukin-1 receptors (NB-LRR-TIR), and nucleotide-binding site-leucine-rich receptor-coiled coil (NB-LRR-CC; Table S4).

3.5.2 | Genes involved in signal transduction

During pathogen infection, at least eight genes showing significant changes in transcript levels were identified as kinases potentially involved in signal transduction, including various mitogen-activated protein kinases. A group of 17 genes were identified as calcium-related or calcium-binding proteins, some of which showed remarkable induction at different sampling times during disease development (Table S5).

3.5.3 | Transcription factors

Of the 1,696 DEGs, 108 were identified as TFs, and 89 of them were annotated with GO term "transcription factor activity" (GO:0003700). No significant enrichment was identified for this GO term during global functional analysis. However, specific analysis

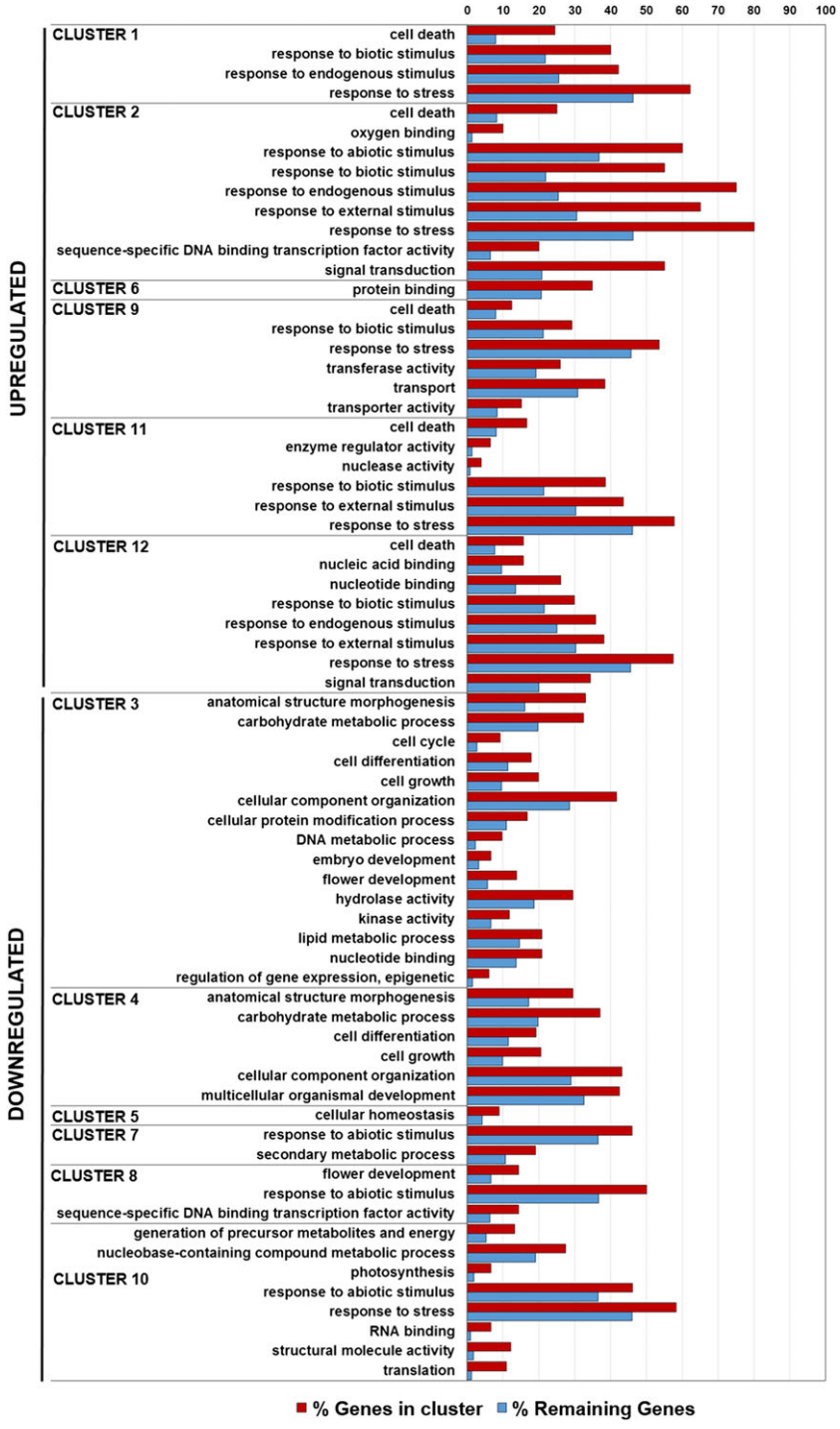

FIGURE 4 Gene Ontology (GO) term enrichment analysis for each cluster identified during treatment. Percentage of each GO term from differentially expressed genes in each cluster compared with percentage observed in remaining differentially expressed genes identified during treatment. Enrichment was significant at $p < .05$

within this group showed a significant enrichment in specific families such as WRKY TF, ethylene-responsive TF, and nac-domain TF. In addition, more than 80% of the members from these three families were overexpressed during the response to the pathogen. In other families such as dehydration-responsive element-binding protein or heat stress TF, most of the members included in the array were also identified as DEGs (Figure S2). Seventy-one TFs presented increased transcript levels at one or more sampling times during disease development. An nac-domain TF reached the highest induction for TFs at 14 dpi (Table S6).

3.5.4 | Genes involved in defence

A group of induced DEGs was related to regulation mediated by SA. Two up-regulated genes, isotig02962 and isotig10240, annotated as *senescence-associated carboxylesterase 101-like* (*SAG101*), are homologous to *Arabidopsis thaliana enhanced disease susceptibility 1* (*EDS1*) and *phytoalexin deficient 4* (*PAD4*), respectively, genes acting as molecular players in SA pathways. Three correspond to genes identified as SA-binding proteins. Isotig11511 was significantly induced in the days immediately following inoculation (7 and 4 dpi) and was annotated as npr1 nim1-interacting

TABLE 3 Top 25 up-regulated and down-regulated *Ulmus minor* genes during *Ophiostoma novo-ulmi* invasion

Isotig *Ulmus minor*	Locus TAIR	Description Blast2GO	Cluster number	Fold change				
				Day 1	Day 3	Day 7	Day 14	Day 21
Up-regulated genes								
isotig11262	*AT4G16260*	Glucan endo-beta-glucosidase-like	C1			4.26	5.80	350.16
isotig04787	*AT3G04720*	Wound-induced protein win2	C11				3.08	331.87
isotig05804	*AT1G20030*	Thaumatin-like protein 1a-like	C11				3.45	250.26
isotig07572	*AT3G57240*	Glucan endo-beta-glucosidase-like	C1		4.13	32.78	180.21	90.08
isotig17580	*AT2G15780*	Early nodulin-55-2-like	C1		2.12	13.91	88.57	173.20
isotig03409	*AT5G23960*	Valencene synthase-like	C1				10.06	171.70
isotig10737	*AT2G38540*	Non-specific lipid-transfer protein 1-like	C1		1.90	3.23	4.03	149.82
isotig03346	*AT4G11650*	Thaumatin-like protein	C1		1.72	8.80	8.32	138.64
isotig06808	*AT2G31790*	UDP-glycosyltransferase 74e2-like	C1			4.42	11.25	105.67
isotig11573	-	Uncharacterized protein LOC103431225	C1	3.73	2.00	9.05	26.11	99.30
isotig07125	*AT4G33720*	Basic form of pathogenesis-related protein 1	C11				2.36	92.81
isotig03875	*AT3G54420*	Endochitinase PR4	C11				3.14	92.27
isotig10417	*AT4G16260*	Glucan endo-beta-glucosidase-like	C1			8.34	9.77	88.68
isotig16547	*AT1G78780*	Pathogen-related protein	C1			5.52	21.29	86.92
isotig04903	*AT1G23740*	2-methylene-furan-3-one reductase-like	C1	2.55	4.02	22.38	36.08	81.62
isotig03269	-	Uncharacterized protein LOC100500233	C1			13.42	14.89	81.11
isotig05411	*AT1G17860*	Miraculin-like	C11					77.68
isotig13869	*AT2G15220*	Plant basic secretory family protein	C1			4.69	6.77	72.52
isotig13833	*AT5G05340*	Cationic peroxidase 1-like	C1			12.10	66.85	46.58
isotig09759	*AT3G04720*	Wound-induced protein win2	C11				5.46	65.26
isotig05385	*AT4G11650*	Pathogenesis-related protein 5-like	C1			18.03	62.78	65.13
isotig18444	*AT5G24090*	Acidic endochitinase-like	C11					62.26
isotig00944	-	Hypothetical protein POPTR_0391s00200g	C1	2.20	4.42	27.60	38.61	59.84
isotig14143	*AT2G37040*	Phenylalanine ammonia-lyase-like	C1	5.10	2.60	4.57	29.19	59.84
isotig19956	*AT1G55290*	Feruloyl ortho-hydroxylase 1-like	C1			6.51	10.48	52.43
Downregulated genes								
isotig20170	*AT3G15050*	Protein IQ-domain 1-like	C4			−2.23	−2.27	−23.47
isotig06390	*AT3G01670*	Uncharacterized protein LOC103403085	C4					−23.70
isotig04495	*AT2G34700*	Pistil-specific extension-like protein	C4					−24.22
isotig04288	*AT5G23860*	Tubulin beta-1 chain-like	C4		−2.28	−2.31		−25.61
isotig03459	-	NA	C4		2.17		−5.49	−26.54
isotig13117	*AT5G22580*	Probable protein Pop3	C4		−1.79			−27.65
isotig05650	*AT1G70830*	MLP-like protein 28	C4				−2.99	−28.05
isotig02193	-	NA	C4	−1.95	−1.98			−28.34
isotig19984	*AT1G80760*	Probable aquaporin NIP5-1	C4		2.57		−9.36	−28.41
isotig07820	*AT1G72230*	Blue copper	C4				−2.15	−29.06
isotig18583	-	NA	C4				−4.73	−29.34
isotig09549	*AT5G03170*	Fasciclin-like arabinogalactan protein 11-like	C4		−2.63	−2.76	−2.82	−30.24
isotig14055	-	NA	C4		−3.11	−3.85	−2.87	−35.89
isotig06823	-	Hypothetical protein L484_012049	C4	−1.97			−3.75	−41.30
isotig09181	*AT3G53980*	Protease inhibitor seed storage lipid-transfer protein family protein	C4	2.33	5.49		−9.05	−48.31
isotig13006	-	NA	C4	−1.96			−11.45	−52.26
isotig10675	*AT5G60490*	Fasciclin-like arabinogalactan protein 11-like	C4		−2.42	−2.24	−2.38	−58.96
isotig15736	-	NA	C2		5.95	−62.53	2.16	
isotig18819	*AT1G44760*	Adenine nucleotide alpha hydrolases-like	C4			−2.58	−6.16	−67.20
isotig06717	*AT5G03170*	Fasciclin-like arabinogalactan protein 11-like	C4	−2.20	−3.28	−4.92	−4.51	−81.23
isotig08263	*AT5G60490*	Fasciclin-like AGP 15 family protein	C4	−2.05	−2.77	−4.94	−4.78	−100.53
isotig02686	*AT2G24210*	(−)-germacrene D synthase	C4		2.05		−5.63	−107.26
isotig13757	*AT5G60490*	Fasciclin-like AGP 15 family protein	C4	−1.88	−2.78	−5.06	−5.32	−108.72
isotig13675	-	NA	C4	−1.92	−2.68	−5.51	−6.82	−137.26
isotig18734	-	NA	C2	7.22	13.95	−172.13		6.69

Note. Locus TAIR indicates protein from *Arabidopsis thaliana* showing highest homology with the *Ulmus minor* sequence. For determination of significance, see Section 2.

protein, which is potentially involved in late regulation of SAR (Table S7).

Forty-eight genes from *U. minor* with significant induction were identified as members of different PR protein families. A remarkable increase in transcript levels was observed in members of certain families, mainly in *PR2*-type (glucan endo-beta-glucosidases), *PR4*-type (chitinases), *PR5*-type (thaumatin), *PR9*-type (peroxidases), and *PR14*-type (non-specific lipid transfer proteins). Notable overexpression was observed in some genes included in the unclassified PR proteins group, for example, an early nodulin, a late embryogenesis abundant hydroxyproline-rich glycoprotein, and an α-amylase (Table S8).

Another group of induced genes, catalogued as transporters, showed the highest induction in genes involved in polyols, ammonium, sugars, and zinc transport. Numerous genes encoding ATP binding cassette (ABC) transporters also showed remarkable increase in transcript levels. Genes related to biotic stress response (*major allergen* or some *gdsl esterase lipase* genes) showed significantly increased transcript levels. Moderate variation in transcript levels, usually down-regulated during *O. novo-ulmi* invasion, was observed in seven genes that presented homology with *WAT1* (*Walls are Thin1*) gene from *A. thaliana* (Table S7).

3.6 | Pathways correlated with disease development

Genes encoding enzymes involved in various pathways included in KEGG were analysed globally to identify specific metabolic pathways correlated with disease development. A pathway is considered significantly enriched when a group of genes encoding enzymes in the pathway are positively or negatively correlated with the main trend observed in expression patterns. A group of metabolic processes with significant enrichment ($p < .05$) were identified during the analysis (Figure 5 and Table S9).

Twelve of the metabolic pathways identified were increasingly up-regulated over time. The pathways included biosynthesis of terpenoids, anthocyanins, flavonoids, isoquinoline alkaloids, and indole alkaloids, as well as metabolism of butanoate, propanoate, and glyoxylate and dicarboxylate.

Pathways related to metabolism of amino acids such as valine, alanine, and tyrosine were also significantly enriched. Four pathways were down-regulated over time, mainly showing repression in enzymes related to pentose and glucuronate interconversions, starch and sucrose metabolism, sphingolipid metabolism, and fatty acid biosynthesis.

3.7 | Validation of microarray data by RT-PCR

To validate the microarray results, quantitative RT-PCR was performed to determine the expression levels of eight *Ulmus* genes selected to cover several functional groups and expression patterns from the list of DEGs in response to *O. novo-ulmi*. RT-PCR confirmed the microarray expression patterns (Figure 6). Seven of the eight genes analysed showed a Pearson's correlation value higher than 0.9, including values close to 1 in some genes. Only one gene showed a lower Pearson's correlation value (0.6), which could be attributed to the different dynamic range of the two techniques.

4 | DISCUSSION

The main objective of this work was to characterize the expression profiles of plant defence genes in *U. minor* over the time course of vessel invasion by *O. novo-ulmi*, the causal agent of DED. We examined the Atinian elm, also known as English elm, an iconic tree widely distributed throughout Europe since Roman times. This clone is known to be highly susceptible to *O. novo-ulmi* attack (Martín, Solla, Coimbra, & Gil, 2008), as confirmed in this experiment. Inoculated plants showed severe wilting and almost total canopy desiccation by the end of the observation period (120 dpi). The evolution of the disease has been correlated to physiological parameters such as water potentials, gas exchange, and hydraulic conductance, all of which decreased drastically for this clone in infected compared to control plants (Li et al., 2016). This study focuses on the molecular response of this clone to DED and the influence of its xylem anatomical traits.

The anatomical structure of Atinian elm is perfectly adapted to maximize hydraulic conductance in early spring. The earlywood conducting system is formed almost exclusively of wide earlywood vessels, endowing it with high THC values. In 3-year-old branches, THC values are particularly high in Atinian elm compared to values in elms tolerant to *O. novo-ulmi* (Table 2) and other susceptible clones (Martín, Solla, Esteban, de Palacios, & Gil, 2009; Venturas et al., 2014). Anatomical structure probably contributes to the high susceptibility of the clone to *O. novo-ulmi*, favouring the spread of fungal bud cells, toxins, and cell wall-degrading enzymes, ultimately leading to vessel occlusion and/or embolism. The large pit apertures in the clone could also facilitate the spread of fungal products in the xylem sap and penetration of the pit membrane by fungal hyphae (Martín et al., 2009). The high proportion of ray parenchyma cells is important, because this tissue has a decisive role in (a) exudation of tyloses, gels, and gums into the vessels through pit connections (Figure 2; Chattaway, 1949) and (b) storage of nonstructural carbohydrates (NSCs; Magel, Jay-Allemand, & Ziegler, 1994; Martín et al., 2008). In relation to tylose formation, a strong reaction of the Atinian elm to *O. novo-ulmi* inoculation was detected in cross sections at 120 dpi, with a large proportion of earlywood vessels occluded by tyloses and gums (Figure 2). This reaction corresponds to Wall 1 of the CODIT model (Shigo & Marx, 1977) and may restrict upward and downward movement of the pathogen. However, this reaction can be so efficient that vertical sap transport to the canopy becomes blocked, contributing to tree death (Ouellette, Rioux, Simard, & Cherif, 2004). Therefore, the higher proportion of ray cells in the Atinian elm than in tolerant elms could give this clone greater ability to block vessels that are infected or near infected tissue. The anatomical structure of Atinian elm also suggests a high storage capacity of NSCs in medullary rays, possibly related to the great capability of this clone to occlude vessels with tyloses and gels or gums. These components include accumulation of suberin and polyphenolic compounds, which are formed from stored NSCs and are toxic to microbes (Shain, 1979). NSCs can, however, be a source of easily assimilable metabolites for fungal growth

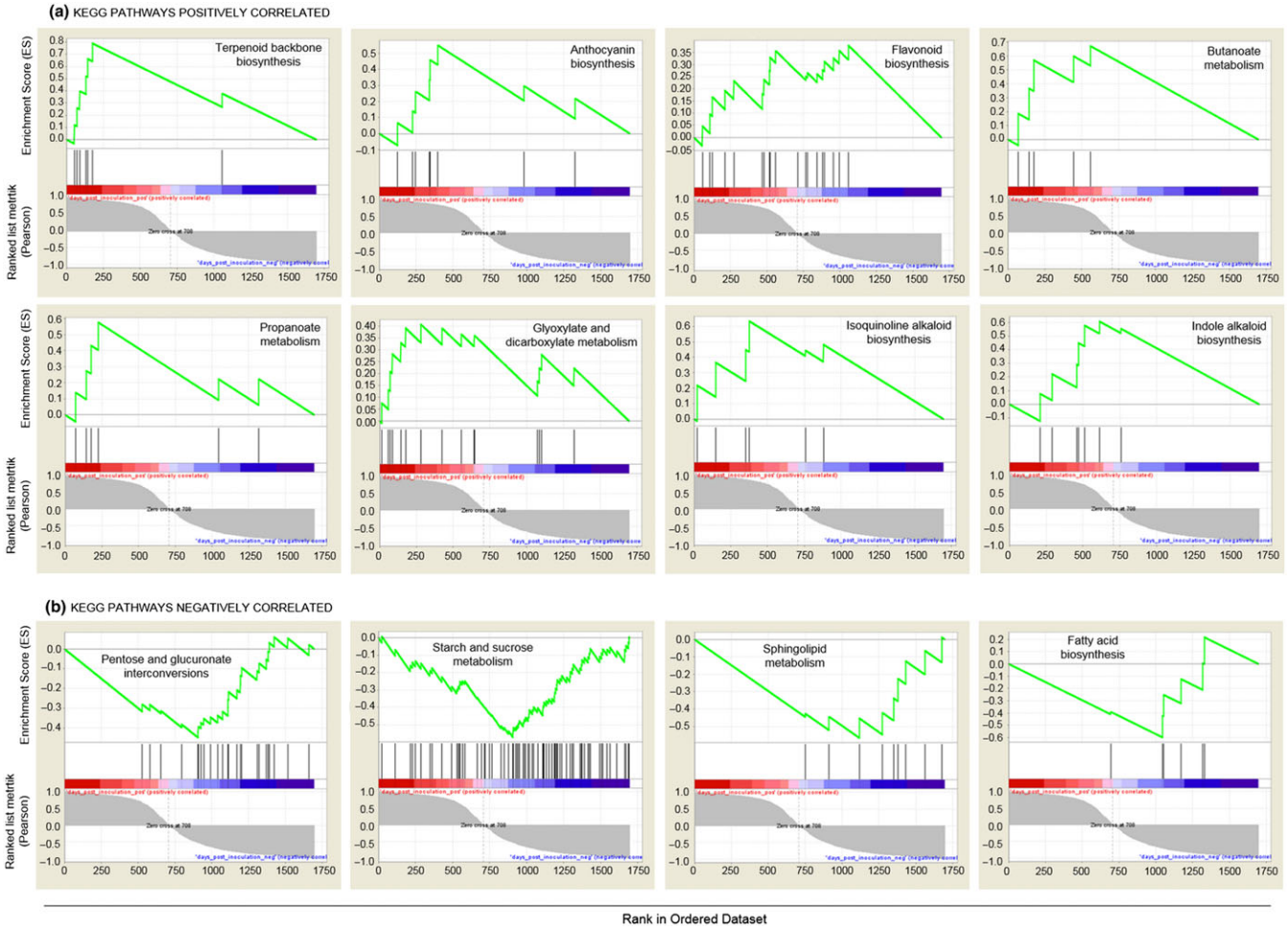

FIGURE 5 Enrichment plot of Kyoto Encyclopedia of Genes and Genomes (KEGG) pathways showing significant changes in gene expression levels of enzyme encoded genes during *Ophiostoma novo-ulmi* invasion. Pathways positively (a) and negatively (b) correlated with expression value during time course analysis. Pathways were selected when $p < .05$. Green lines show enrichment profiles. Vertical black lines indicate the position of each gene in ranked list

once the fungus is able to penetrate living cells (Martín et al., 2009; Ouellette, 2008). Despite uncertainty as to the exact role of xylem parenchyma cells in DED pathogenesis, these tissues may be responsible for major defence responses triggered in an attempt to compartmentalize the DED pathogen.

Relationships between vascular wilt pathogens and their host plants are complicated to study because they take place inside plants, usually in specific niches (e.g., conducting elements). From a molecular perspective, response to wilt pathogens triggers activation of the plant immune system and induction or repression of specific genes in wilt pathogen-infected tissues (Yadeta & Thomma, 2013, and references therein). Therefore, the molecular response of *U. minor* to *O. novo-ulmi* should induce common and specific patterns during disease development. To date, arguably the most in-depth molecular study analysing the DED pathosystem was performed by Aoun, Jacobi, Boyle, and Bernier (2010) using *in vitro* interactions between *Ulmus americana* cells and *O. novo-ulmi* to identify a set of DEGs. An interesting group of transcripts were identified, some of which have recently been searched for in mature trees to analyse their putative relationship with DED tolerance (Sherif et al., 2016). Using high-throughput sequencing, the genetic information available for *Ulmus* spp. has been considerably increased with the creation of an EST library in response to feeding or methyl jasmonates (Büchel et al., 2012) and a *U. minor* transcriptome in response to abiotic stress (drought) and biotic stresses (including inoculation with *Ophiostoma* spp. and other pathogens; Perdiguero et al., 2015a, 2015b). However, to be able to identify genes of interest in these libraries, it is necessary to conduct differential expression analysis focussing on a specific problem.

Herein, we report 1,696 DEGs during *O. novo-ulmi* invasion, of which 89 % showed homology with proteins from a set of plant model species contained in RefSeq database according to the *U. minor* transcriptome used as reference (Perdiguero et al., 2015a). Using clustering analysis, DEGs were grouped into 12 clusters with shared expression patterns. This approach could be a basis for constructing useful coexpression networks highlighting putative protein–protein interactions during *O. novo-ulmi* invasion. Interestingly, coherence was identified in results from functional enrichment analysis. Clusters showing up-regulation in expression patterns were associated with GO terms "response to biotic stimulus" and "response to stress," and also "cell death," the final consequence of immune system activation (Jones & Dangl, 2006). Enrichment shown by Cluster 2, including the terms "oxygen binding," "sequence-specific DNA binding transcription factor," and "signal transduction," coincident with high induction 24 h post inoculation, indicates rapid activation of molecular response to the

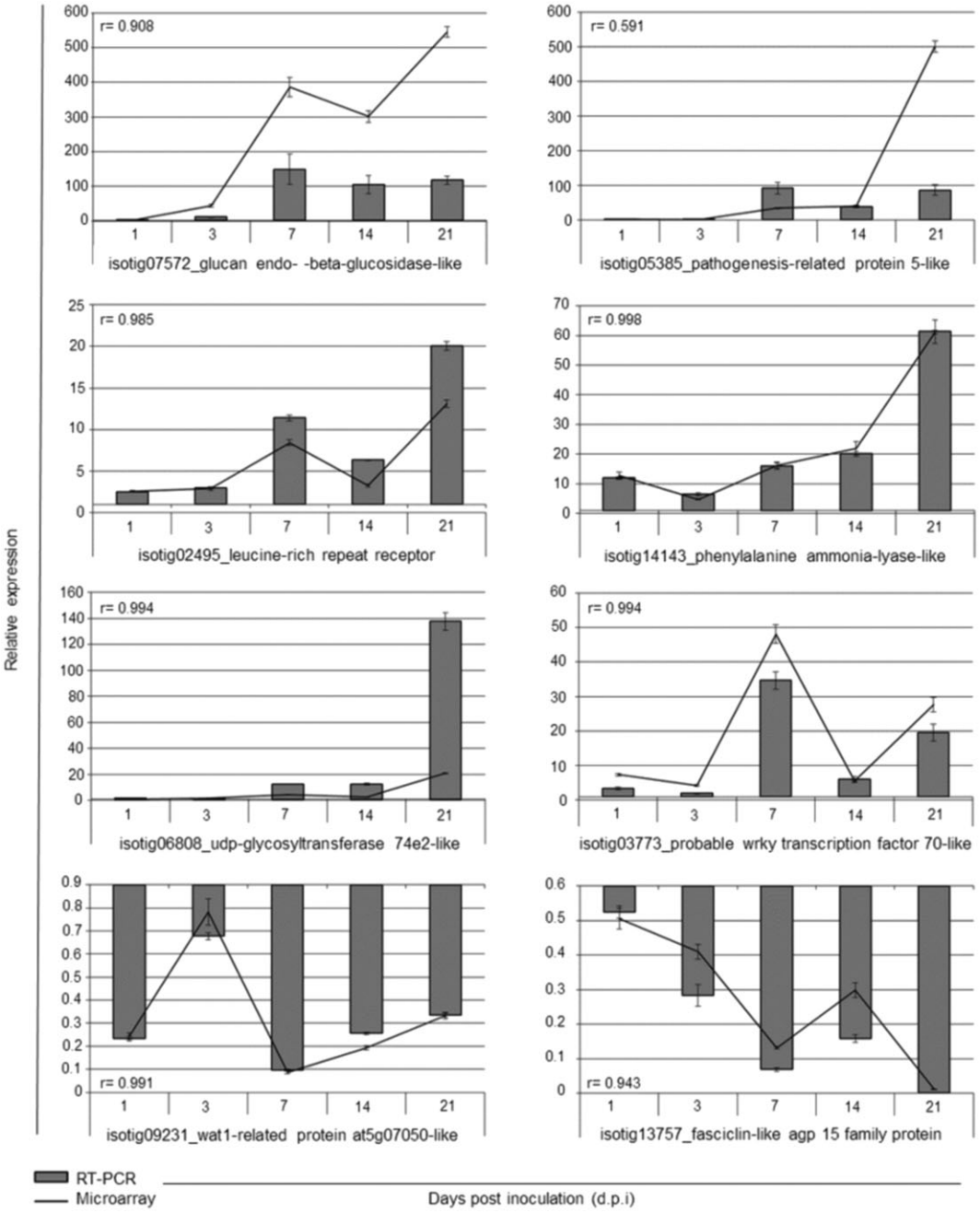

FIGURE 6 Validation of microarrays by reverse transcription polymerase chain reaction (RT-PCR). Expression profiles obtained with microarray (bars) and RT-PCR techniques (continuous line) for eight selected differentially expressed genes. Pearson's correlation (*r*) between techniques is indicated for each gene in each panel

presence of the pathogen even at considerable distance from the pathogen entry point: Branches collected for the study had a healthy appearance and were 2 m from the inoculation point.

The immune system of infected plants produces plant hormones that actively regulate response to infection by controlling signalling pathways. SA is a signal molecule required for SAR. It is a generally observed pattern that SA regulates resistance to biotrophs and hemibiotrophs, whereas JA regulates resistance to necrotrophs (Pieterse et al., 2009). *O. novo-ulmi* is considered a hemibiotroph, and therefore, an SA predominant response should be expected, although both types of plant resistance responses could be involved. SA and JA accumulations have been reported in *U. americana* plants inoculated with *O. novo-ulmi* (Sherif et al., 2016). In the molecular response of Atinian elm, overexpression of genes related to SAR to pathogens from 7 to 21 dpi is noteworthy. These SAR-related genes also showed a progressive increase in expression over time. This response to pathogens (generally bacteria or fungi) has been widely described in other plants and is dependent on SA (Vlot, Dempsey, & Klessig, 2009). After localized pathogen infection, several signals are triggered in distal parts of the plant to enhance defence against invasion in the entire plant. In our study, we found several up-regulated genes with high homology to SAR-related genes described in *Arabidopsis*. These genes are mainly grouped in Clusters 1 and 11 (Table S3). Isotig02962 and isotig10240, homologous to *EDS1* and *PAD4*, respectively, showed similar changes in expression at the same sampling times. Isotig03130, homologous to *SAG101*, also showed a significant increase in transcript levels from

7 to 20 dpi. This situation corresponds precisely to the common SAR response described in other plants infected by fungal pathogens. In *A. thaliana* infected by *Fusarium graminearum*, proteins EDS1, PAD4, and SAG101 act in a complex that promotes SA accumulation and, therefore, SA-mediated defence, limiting infection by the pathogen (Makandar et al., 2015). In this complex, EDS1 is essential to recognize pathogens through R proteins and, consequently, triggers resistance at pathogen infection foci (Feys, Moisan, Newman, & Parker, 2001). EDS1 and PAD4 are partners in basal resistance to various pathogens. These proteins are regulators of ETI, which is mediated by resistance (*R*) genes (Feys et al., 2005). In our analysis, several isotigs were annotated as genes involved in this signalling pathway (Table S4). Genes coding for LRRs or TIRs were principally induced in *Ophiostoma*-inoculated trees from 7 dpi onwards, and this activation coincides with increased expression of SAR-marked genes, such as *phenylalanine ammonia-lyase* and *PR* genes (Table 3). These genes have been described as overexpressed during DED development (Aoun et al., 2009; Nasmith et al., 2008) and were the most up-regulated genes in our study. Seven of the 25 top up-regulated genes (Table 3) were identified by Aoun et al. (2010) in *U. americana* callus.

In the classic SAR response, activation of *PR* genes contributes to enhance whole-plant resistance (Pieterse et al., 2014). Several genes annotated as *PR* were found with high and progressively increased expression from 3 or 7 dpi to 21 dpi in inoculated trees. We highlight the up-regulation of genes with homology to *Arabidopsis* PR proteins, such as PR2 with β-1,3-glucanase activity, several chitinases and PR4, thaumatin-like proteins belonging to the PR5 family, and non-specific lipid transfer proteins classified as PR14 (Table S8). Although PR1 is a good marker of SAR, its function is still unknown; however, the other PR families are all proteins with antifungal activity (Van Loon & Van Strien, 1999). We therefore confirmed that inoculation with *O. novo-ulmi* triggered activation of several genes encoding antifungal activities in distal tissues in VA-AP38.

This activation occurred with increased expression of various WRKY TFs directly related to SAR regulation. Homologs to *WRKY18*, *WRKY40*, and *WRKY70* appeared up-regulated in *Ophiostoma*-inoculated trees; these three TFs are positive regulators of SA-mediated defence and negative regulators of JA-mediated responses (Hu, Dong, & Yu, 2012; Pandey, Roccaro, Schön, Logemann, & Somssich, 2010). We also found a TF homologous to *WRKY33* that regulates camalexin biosynthesis by inducing genes of this pathway, including various *CYP71* genes (cytochrome p450 with monooxygenase activity; Mao et al., 2011) that were also up-regulated in this study (Clusters 1 and 11).

Enrichment analysis using pathways permitted identification of interesting processes during *O. novo-ulmi* invasion. The significant up-regulation observed in biosynthesis of terpenoids matched the accumulation of lignin, and the up-regulation of anthocyanin and flavonoid biosynthesis was consistent with accumulation of phenolic compounds (i.e., in vessel lumina for restricting axial movement of the pathogen), both reported in *U. minor* trees after *O. novo-ulmi* infection (Martín et al., 2007, 2008; Ouellette et al., 2004).

Several up-regulated genes associated with oxidative stress were identified at 14 and 21 dpi (Clusters 9 and 12). Genes encoding peroxidases, glutaredoxins, glutathione S-transferases, and nac-TFs are expressed at these sampling times, indicating an increase in oxidative stress induced by the pathogen. As there was no evidence of pathogen presence at the sampling time, a hypothetical situation could be explained by an increase of signalling mediated by ROS. These ROS are produced mainly by the NADPH oxidases in walls of cells in direct contact with the pathogen. This process leads to great increases in the superoxide anion (O_2^-), which is reduced to H_2O_2 by superoxide dismutases. H_2O_2 can diffuse into cells and move long distances, acting as a signal with SA and nitric oxide in many defence mechanisms in plants (Mittler, 2002).

Clusters with down-regulated genes (not previously analysed in other elm studies) showed functionalities related to growth or anatomical structure and morphogenesis. These changes reflect differences in the energy use strategy of infected plants. In the absence of virulent pathogens, plants invest energy in growth, but when their physiological functions are challenged by virulent pathogens, they use energy to form defence structures and substances (Huot, Yao, Montgomery, & He, 2014). A group of strongly repressed genes (Cluster 4) encoded FLAs that appear to contribute specifically to the biomechanical properties of stems through their impact on the synthesis and architecture of the secondary cell wall. Analyses with inactivated or mutant FLA transgenic plants (MacMillan, Mansfield, Stachurski, Evans, & Southerton, 2010; Wang et al., 2015) showed down-regulation of some xylem-specific genes involved in cell wall formation that resulted in altered stem biomechanics of transgenic plants. In view of the key role of FLA in stem composition and biomechanics, we hypothesize that strong down-regulation during disease development favoured invasion of vessels by the pathogen.

Among down-regulated pathways, pentose and glucuronate interconversions and starch and sucrose metabolism are represented by numerous groups of genes involved in starch formation and regulation of pectin esterification. Both processes are important in cell wall development and defence responses. This discovery, along with other down-regulated genes related to secondary metabolism, lipid metabolism, and cellular cycle processes, suggests that the SAR response is directly associated with a decrease in development, differentiation, and vegetative growth. These results agree with earlier research demonstrating depletion of *U. minor* starch reserves during *O. novo-ulmi* infection, which was more intense in susceptible than in resistant genotypes (Martín, Solla, Coimbra, & Gil, 2005).

The down-regulation of genes related to auxin and gibberellin signalling pathways (Clusters 5, 7, and 8) in *Ophiostoma*-inoculated trees from 14 to 21 dpi is noteworthy. It is well known that these hormones control growth in plants by promoting induction of a large number of growth-related genes (Davies, 2010). However, some pathogens also produce auxins or manipulate auxin biosynthesis in plants. To avoid pathogen growth, plants produce SA to repress the auxin and gibberellin signalling pathways and stabilize auxin response repressors as part of the defence mechanisms (Wang, Pajerowska-Mukhtar, Culler, & Dong, 2007). The repressed auxin-related genes found in our study could be a direct antagonistic effect of SAR in trees inoculated with *O. novo-ulmi*.

Identification and classification of defence-related genes are considered a task of primary importance for the forest research community (Kovalchuk et al., 2013). This work is a first global overview

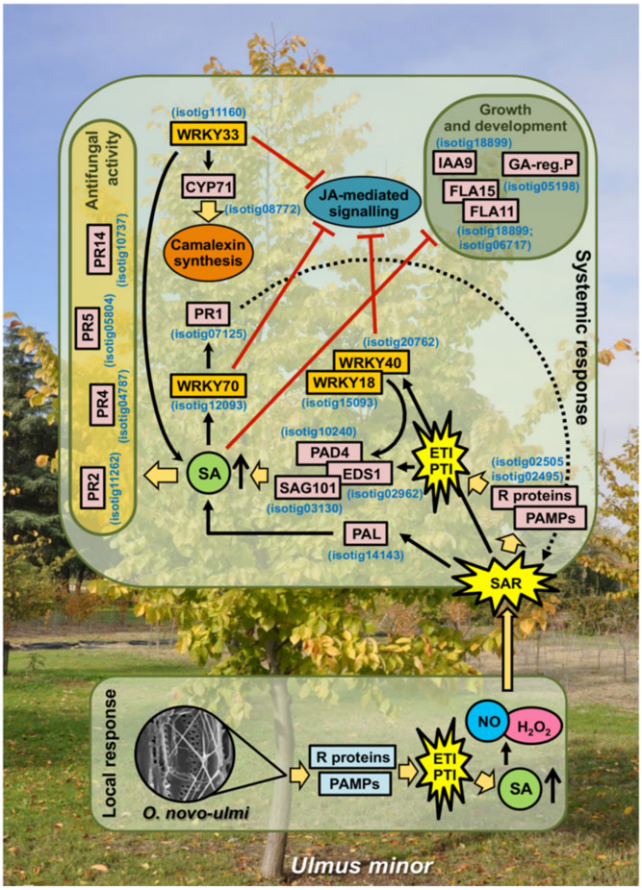

FIGURE 7 Schematic representation of putative molecular responses in Atinian elms inoculated with *Ophiostoma novo-ulmi*. Inoculation at the base of the *Ulmus minor* trunk induces a local response where pathogen-associated molecular patterns (PAMPs) and resistance (R) proteins are expressed, generating two resistance responses: effector-triggered immunity (ETI) and PAMP-triggered immunity (PTI). This process activates the salicylic acid (SA) pathway in the affected area and a similar rapid response in distal parts of the tree through signalling by SA and reactive oxygen species such as nitric oxide (NO) and hydrogen peroxide (H_2O_2). This response in distal healthy tissues is known as systemic acquired resistance (SAR). The systemic response activates pathways involved in the increase of SA levels through induction of the first enzyme in the phenylpropanoid pathway (phenylalanine ammonia lyase; PAL) and the combined action of three proteins: senescence-associated carboxylesterase 101-like (SAG101), enhanced disease susceptibility 1 (EDS1), and phytoalexin deficient 4 (PAD4). This complex is regulated by two transcription factors, WRKY18 and WRKY40. Increased SA levels activate the expression of pathogenesis-related genes (*PR*) that codify for different proteins with antifungal activity, whereas SA-related pathways down-regulate genes involved in jasmonic acid (JA)-mediated signalling and growth and development. Some of these genes are related to the actions of other phytohormones such as auxins and gibberellins, for example, indoleacetic acid-induced protein 9 (IAA9) and gibberellin (GA)-regulated protein, whereas others are directly involved in plant development, for example, the fasciclin-like arabinogalactan proteins (FLAs). In the systemic response, other pathways are induced, producing positive feedback on SA-related pathways and suppressing JA-related pathways, as with camalexin synthesis regulated by transcription factor WRKY33 and a cytochrome p450 of the CYP71 family

of the molecular response of *U. minor* saplings to xylem invasion by *O. novo-ulmi*. The DEGs reported in this analysis are the first expression level study in elm saplings infected with *O. novo-ulmi*. Among these DEGs, a significant number of genes were identified across the steps that occur during plant immune system activation. Numerous genes potentially involved in perception, signal transduction, and transcription modulation, as well as defence genes, were identified and analysed. The results highlight several receptors, kinases, and TFs in various families that are certain to provide interesting material for advancing knowledge of the DED pathosystem. Based on the results of this study, Figure 7 shows a putative model of a systemic response induced in *U. minor* inoculated with *O. novo-ulmi* and highlights pathways with greater differential expression between inoculated and control plants.

A considerable number of the DEGs reported are homologous to genes that have been described as key regulators during plant–pathogen interactions in other species, including interesting genes identified in other wilt diseases (Yadeta & Thomma, 2013). For instance, *WAT1* encodes a tonoplast localized auxin transporter that has been associated with resistance to vascular pathogens in *A. thaliana*, including the fungus *Verticillium dahliae* (Denancé et al., 2013). A large group of genes with remarkable up- or down-regulation during disease development showed no homology to proteins from other plants. These genes pose new challenges for researchers interested in identifying specific genes involved in wilt diseases of trees or specifically involved in *Ulmus* sp. and *O. novo-ulmi* interaction. Most of the up-regulated and down-regulated genes found in this study indicate that the response in healthy branches located distally from the inoculation point resembles the general SAR responses described for plant defence. Gruner, Griebel, Návarová, Attaran, and Zeier (2013) presented an in-depth study showing all the up- and down-regulated genes in SAR-associated defence in *Arabidopsis* against *Pseudomonas syringae*. Their work strongly supports our data, because many of the genes described in *Arabidopsis* were found here in *U. minor*. Our results support our initial hypotheses, because the pathogen promoted a systemic response in distal parts of the plant, and this response corresponded with the typical SAR mediated by SA. In order to determine the traits behind the high susceptibility of this clone to *O. novo-ulmi*, analyses of tissues in the vicinity of the inoculation point are needed to clearly discern the differences between early local response and systemic responses. Possibly, factors such as the timing and intensity of the local defence responses are crucial to determine the degree of susceptibility to the pathogen. The described anatomical structure of this clone probably contributed to its high susceptibility, favouring pathogen spread in vascular tissues. Our results significantly advance knowledge of vascular diseases of trees and the plant defence mechanism against pathogens. This knowledge is crucial in advancing towards molecular assisted techniques to select and breed trees resistant to vascular pathogens.

ACKNOWLEDGMENTS

We would like to thank Jorge Dominguez and David Medel for preparation of plant material and fungal strains, and Elena Zafra for microsatellite amplification. We would also like to express our

gratitude to the Spanish Elm Breeding and Conservation Programme for supporting this study. This research was funded by the Ministerio de Agricultura, Alimentación y Medio Ambiente (MAGRAMA) and the Spanish National Research Plan (AGL2012-35580 and AGL2015-66925-R MINECO/FEDER, UE). P.P. acknowledges funding from the People Programme (Marie Curie Actions) of the European Union's Seventh Framework Programme (FP7/2007-2013) under REA grant agreement PIEF-GA-2013-627761.

CONFLICT OF INTEREST

The authors have no conflict of interest to declare.

ORCID

Pedro Perdiguero http://orcid.org/0000-0002-5471-9550

REFERENCES

Adie, B. A. T., Pérez-Pérez, J., Pérez-Pérez, M. M., Godoy, M., Sánchez-Serrano, J. J., Schmelz, E. A., & Solano, R. (2007). ABA is an essential signal for plant resistance to pathogens affecting JA biosynthesis and the activation of defenses in *Arabidopsis*. *The Plant Cell*, *19*, 1665–1681.

Al-Shahrour, F., Díaz-Uriarte, R., & Dopazo, J. (2004). FatiGO: A web tool for finding significant associations of Gene Ontology terms with groups of genes. *Bioinformatics*, *20*, 578–580.

Anderbrant, O., Yuvaraj, J., Martin, J., Gil, L., & Witzell, J. (2017). Feeding by *Scolytus* bark beetles to test for differently susceptible elm varieties. *Journal of Applied Entomology*, *141*(5), 417–420.

Aoun, M., Jacobi, V., Boyle, B., & Bernier, L. (2010). Identification and monitoring of *Ulmus americana* transcripts during in vitro interactions with the Dutch elm disease pathogen *Ophiostoma novo-ulmi*. *Physiological and Molecular Plant Pathology*, *74*, 254–266.

Aoun, M., Rioux, D., Simard, M., & Bernier, L. (2009). Fungal colonization and host defense reactions in *Ulmus americana* callus cultures inoculated with *Ophiostoma novo-ulmi*. *Phytopathology*, *99*, 642–650.

Bernier, L., Aoun, M., Bouvet, G., Comeau, A., Dufour, J., Naruzawa, E., … Plourde, K. (2015). Genomics of the Dutch elm disease pathosystem: Are we there yet? *iForest-Biogeosciences and Forestry*, *8*, 149–157.

Brasier, C. M. (2000). Intercontinental spread and continuing evolution of the Dutch elm disease pathogens. In C.P. Dunn (Ed.), *The Elms: breeding, conservation and diseasemanagement* (pp. 61–72). Boston, MA: Springer.

Breitling, R., Armengaud, P., Amtmann, A., & Herzyk, P. (2004). Rank products: A simple, yet powerful, new method to detect differentially regulated genes in replicated microarray experiments. *FEBS Letters*, *573*, 83–92.

Büchel, K., McDowell, E., Nelson, W., Descour, A., Gershenzon, J., Hilker, M., … Meiners, T. (2012). An elm EST database for identifying leaf beetle egg-induced defense genes. *BMC Genomics*, *13*, 242.

Chang, S., Puryear, J., & Cairney, J. (1993). A simple and efficient method for isolating RNA from pine trees. *Plant Molecular Biology Reporter*, *11*, 113–116.

Chattaway, M. M. (1949). The development of tyloses and secretion of gum in·heartwood formation. *Australian Journal of Biological Sciences*, *2*, 227–240.

Davies, P. J. (2010). The plant hormones: Their nature, occurrence, and functions. In P. J. Davies (Ed.), *Plant hormones: Biosynthesis, signal transduction, action!* (pp. 1–15). Dordrecht: Springer Netherlands.

Denancé, N., Ranocha, P., Oria, N., Barlet, X., Rivière, M. P., Yadeta, K. A., … Goffner, D. (2013). Arabidopsis *wat1* (*walls are thin1*)-mediated resistance to the bacterial vascular pathogen, *Ralstonia solanacearum*, is accompanied by cross-regulation of salicylic acid and tryptophan metabolism. *The Plant Journal*, *73*, 225–239.

Domínguez Lerena, S. (2002). Lucha contra una condena letal: La grafiosis está provocando la extinción del olmo en todo el mundo. *Ambienta: La revista del Ministerio de Medio Ambiente*, *14*, 35–40.

Dumolin, S., Demesure, B., & Petit, R. (1995). Inheritance of chloroplast and mitochondrial genomes in pedunculate oak investigated with an efficient PCR method. *Theoretical and Applied Genetics*, *91*, 1253–1256.

Dunn, C. P. (2000). In C.P. Dunn (Ed.), *The Elms: breeding, conservation and disease management*. Boston, MA: Springer.

Ellison, A. M., Bank, M. S., Clinton, B. D., Colburn, E. A., Elliott, K., Ford, C. R., … Lovett, G. M. (2005). Loss of foundation species: Consequences for the structure and dynamics of forested ecosystems. *Frontiers in Ecology and the Environment*, *3*, 479–486.

Faccoli M. & Battisti A. (1997) Observations on the transmission of *Ophiostoma ulmi* by the smaller elm bark beetles (*Scolytus spp.*). Paper presented at the Proceedings of a IUFRO Meeting: Integrating Cultural Tactics Into the Management of Bark Beetles and Reforestation Pests, September 1–3, 1996, Vallombrosa, Italy.

Feys, B. J., Moisan, L. J., Newman, M. A., & Parker, J. E. (2001). Direct interaction between the *Arabidopsis* disease resistance signaling proteins, EDS1 and PAD4. *The EMBO Journal*, *20*, 5400–5411.

Feys, B. J., Wiermer, M., Bhat, R. A., Moisan, L. J., Medina-Escobar, N., Neu, C., … Parker, J. E. (2005). *Arabidopsis* SENESCENCE-ASSOCIATED GENE101 stabilizes and signals within an ENHANCED DISEASE SUSCEPTIBILITY1 complex in plant innate immunity. *The Plant Cell*, *17*, 2601–2613.

Gil, L., Fuentes-Utrilla, P., Soto, A., Cervera, M. T., & Collada, C. (2004). English elm is a 2,000-year-old Roman clone. *Nature*, *431*, 1053–1053.

Giordano, R., Salleo, A., Salleo, S., & Wanderlingh, F. (1978). Flow in xylem vessels and Poiseuille's law. *Canadian Journal of Botany*, *56*, 333–338.

Gruner, K., Griebel, T., Návarová, H., Attaran, E., & Zeier, J. (2013). Reprogramming of plants during systemic acquired resistance. *Frontiers in Plant Science*, *4*, 252.

Gururani, M. A., Venkatesh, J., Upadhyaya, C. P., Nookaraju, A., Pandey, S. K., & Park, S. W. (2012). Plant disease resistance genes: Current status and future directions. *Physiological and Molecular Plant Pathology*, *78*, 51–65.

Hong, F., Breitling, R., McEntee, C. W., Wittner, B. S., Nemhauser, J. L., & Chory, J. (2006). RankProd: A bioconductor package for detecting differentially expressed genes in meta-analysis. *Bioinformatics*, *22*, 2825–2827.

Hu, Y., Dong, Q., & Yu, D. (2012). *Arabidopsis* WRKY46 coordinates with WRKY70 and WRKY53 in basal resistance against pathogen *Pseudomonas syringae*. *Plant Science*, *185*, 288–297.

Huot, B., Yao, J., Montgomery, B. L., & He, S. Y. (2014). Growth–defense tradeoffs in plants: A balancing act to optimize fitness. *Molecular Plant*, *7*, 1267–1287.

Jeng, R., Alfenas, A., Hubbes, M., & Dumas, M. (1983). Presence and accumulation of fungitoxic substances against *Ceratocystis ulmi* in *Ulmus americana*: Possible relation to induced resistance. *European Journal of Forest Pathology*, *13*, 239–244.

Jones, J. D., & Dangl, J. L. (2006). The plant immune system. *Nature*, *444*, 323–329.

Kovalchuk, A., Keriö, S., Oghenekaro, A. O., Jaber, E., Raffaello, T., & Asiegbu, F. O. (2013). Antimicrobial defenses and resistance in forest trees: Challenges and perspectives in a genomic era. *Annual Review of Phytopathology*, *51*, 221–244.

Krause, C., Ichida, J., Schreiber, L., & Domir, S. (1996). Host-parasite relationships of susceptible and resistant elm callus cultures challenged with *Ophiostoma ulmi* (Buisman) Nannf. *Journal of Environmental Horticulture*, *14*, 33–38.

Li, M., López, R., Venturas, M., Martín, J. A., Domínguez, J., Gordaliza, G. G., … Rodríguez-Calcerrada, J. (2016). Physiological and biochemical differences among *Ulmus minor* genotypes showing a gradient of resistance to Dutch elm disease. *Forest Pathology*, *46*, 215–228.

MacMillan, C. P., Mansfield, S. D., Stachurski, Z. H., Evans, R., & Southerton, S. G. (2010). Fasciclin-like arabinogalactan proteins: Specialization for stem biomechanics and cell wall architecture in Arabidopsis and *Eucalyptus*. *The Plant Journal*, *62*, 689–703.

Magel, E., Jay-Allemand, C., & Ziegler, H. (1994). Formation of heartwood substances in the stemwood of *Robinia pseudoacacia* L. II. Distribution of nonstructural carbohydrates and wood extractives across the trunk. *Trees*, *8*, 165–171.

Makandar, R., Nalam, V. J., Chowdhury, Z., Sarowar, S., Klossner, G., Lee, H., … Parker, J. E. (2015). The combined action of ENHANCED DISEASE SUSCEPTIBILITY1, PHYTOALEXIN DEFICIENT4, and SENESCENCE-ASSOCIATED101 promotes salicylic acid-mediated defenses to limit *Fusarium graminearum* infection in *Arabidopsis thaliana*. *Molecular Plant-Microbe Interactions*, *28*, 943–953.

Mao, G., Meng, X., Liu, Y., Zheng, Z., Chen, Z., & Zhang, S. (2011). Phosphorylation of a WRKY transcription factor by two pathogen-responsive MAPKs drives phytoalexin biosynthesis in Arabidopsis. *The Plant Cell*, *23*, 1639–1653.

Martín, J., Fuentes-Utrilla, P., & Witzel, J. (2010). Ecological factors in Dutch elm disease complex in Europe—A review. In L. Magnus, J. Brunet, L. Mattson & M. Nylinder (Eds.), *Ecological Bulletins*, *Bulletin 53*, *Broadleaved Forests in Southern Sweden: Management for Multiple Goals* (pp. 209–224). Lund, Sweden: Wiley-Blackwell.

Martín, J., Solla, A., Burón, M., López-Almansa, J., & Gil, L. (2006). Caracterización histórica, ecológica, taxonómica y fitosanitaria de una olmeda relicta en Rivas-Vaciamadrid (Madrid). *Investigación agraria. Sistemas y recursos forestales*, *15*, 208–217.

Martín, J., Solla, A., Coimbra, M., & Gil, L. (2008). Metabolic fingerprinting allows discrimination between *Ulmus pumila* and *U. minor*, and between *U. minor* clones of different susceptibility to Dutch elm disease. *Forest Pathology*, *38*, 244–256.

Martín, J., Solla, A., Woodward, S., & Gil, L. (2007). Detection of differential changes in lignin composition of elm xylem tissues inoculated with *Ophiostoma novo-ulmi* using Fourier transform-infrared spectroscopy. *Forest Pathology*, *37*, 187–191.

Martín, J. A., Solla, A., Coimbra, M. A., & Gil, L. (2005). Metabolic distinction of *Ulmus minor* xylem tissues after inoculation with *Ophiostoma novo-ulmi*. *Phytochemistry*, *66*, 2458–2467.

Martín, J. A., Solla, A., Esteban, L. G., de Palacios, P., & Gil, L. (2009). Bordered pit and ray morphology involvement in elm resistance to *Ophiostoma novo-ulmi*. *Canadian Journal of Forest Research*, *39*, 420–429.

Martín, J. A., Solla, A., Venturas, M., Collada, C., Domínguez, J., Miranda, E., … Gil, L. (2015). Seven *Ulmus minor* clones tolerant to *Ophiostoma novo-ulmi* registered as forest reproductive material in Spain. *iForest-Biogeosciences and Forestry*, *8*, 172–180.

Mittler, R. (2002). Oxidative stress, antioxidants and stress tolerance. *Trends in Plant Science*, *7*, 405–410.

Moore, J. W., Loake, G. J., & Spoel, S. H. (2011). Transcription dynamics in plant immunity. *The Plant Cell*, *23*, 2809–2820.

Nasmith, C., Jeng, R., & Hubbes, M. (2008). A comparison of in vivo targeted gene expression during fungal colonization of DED-susceptible *Ulmus americana*. *Forest Pathology*, *38*, 104–112.

Nordin, J. H., & Strobel, G. A. (1981). Structural and immunochemical studies on the phytotoxic peptidorhamnomannan of *Ceratocystis ulmi*. *Plant Physiology*, *67*, 1208–1213.

Ouellette G.B. (2008) Close-ups on aspects of fungal wilt diseases [online]. Available from www.wilt-ism.net [accessed 5 September 2016].

Ouellette, G. B., Rioux, D., Simard, M., & Cherif, M. (2004). Ultrastructural and cytochemical studies of host and pathogens in some fungal wilt diseases: Retro- and introspection towards a better understanding of DED. *Forest Systems*, *13*, 119–145.

Pandey, S. P., Roccaro, M., Schön, M., Logemann, E., & Somssich, I. E. (2010). Transcriptional reprogramming regulated by WRKY18 and WRKY40 facilitates powdery mildew infection of Arabidopsis. *The Plant Journal*, *64*, 912–923.

Perdiguero P., Venturas M., Cervera M.T., Gil L. & Collada C. (2015a) Data from: Massive sequencing of *Ulmus minor*'s transcriptome provides new molecular tools for a genus under the constant threat of Dutch elm disease. Dryad Digital Repository. http://dx.doi.org/10.5061/dryad.ps837.

Perdiguero, P., Venturas, M., Cervera, M. T., Gil, L., & Collada, C. (2015b). Massive sequencing of *Ulmus minor*'s transcriptome provides new molecular tools for a genus under the constant threat of Dutch elm disease. *Frontiers in Plant Science*, *6*, 541.

Pfaffl, M. W. (2001). A new mathematical model for relative quantification in real-time RT-PCR. *Nucleic Acids Research*, *29*, 6.

Pieterse, C. M., Leon-Reyes, A., Van der Ent, S., & Van Wees, S. C. (2009). Networking by small-molecule hormones in plant immunity. *Nature Chemical Biology*, *5*, 308–316.

Pieterse, C. M., Van der Does, D., Zamioudis, C., Leon-Reyes, A., & Van Wees, S. C. (2012). Hormonal modulation of plant immunity. *Annual Review of Cell and Developmental Biology*, *28*, 489–521.

Pieterse, C. M., Zamioudis, C., Berendsen, R. L., Weller, D. M., Van Wees, S. C., & Bakker, P. A. (2014). Induced systemic resistance by beneficial microbes. *Annual Review of Phytopathology*, *52*, 347–375.

Rioux, D., & Ouellette, G. (1991). Barrier zone formation in host and nonhost trees inoculated with *Ophiostoma ulmi*. *Canadian Journal of Botany*, *69*, 2055–2083.

Saeed, A. I., Bhagabati, N. K., Braisted, J. C., Liang, W., Sharov, V., Howe, E. A., … Quackenbush, J. (2006). TM4 microarray software suite. *Methods in Enzymology*, *411*, 134–193.

Shain, L. (1979). Dynamic responses of differentiated sapwood to injury and infection. *Phytopathology*, *69*, 1143–1147.

Sherif, S. M., Shukla, M. R., Murch, S. J., Bernier, L., & Saxena, P. K. (2016). Simultaneous induction of jasmonic acid and disease-responsive genes signifies tolerance of American elm to Dutch elm disease. *Scientific Reports*, *6*, 21934.

Shigo, A. L., & Marx, H. G. (1977). *Compartmentalization of decayin trees*. Agriculture Information Bulletin, 405. Washington D.C. USA: United States Department of Agriculture Forest Service.

Smyth, G. K. (2004). Linear models and empirical Bayes methods for assessing differential expression in microarray experiments. *Statistical Applications in Genetics and Molecular Biology*, *3*(1), 1–25.

Smyth, G. K., & Speed, T. (2003). Normalization of cDNA microarray data. *Methods*, *31*, 265–273.

Solla, A., Martín, J., Ouellette, G., & Gil, L. (2005). Influence of plant age on symptom development in *Ulmus minor* following inoculation by *Ophiostoma novo-ulmi*. *Plant Disease*, *89*, 1035–1040.

Subramanian, A., Tamayo, P., Mootha, V. K., Mukherjee, S., Ebert, B. L., Gillette, M. A., … Lander, E. S. (2005). Gene set enrichment analysis: A knowledge-based approach for interpreting genome-wide expression profiles. *Proceedings of the National Academy of Sciences of the USA*, *102*, 15545–15550.

Takai, S., & Hiratsuka, Y. (1984). Scanning electron microscope observations of internal symptoms of white elm following *Ceratocystis ulmi* infection and cerato-ulmin treatment. *Canadian Journal of Botany*, *62*, 1365–1371.

Van Loon, L., & Van Strien, E. (1999). The families of pathogenesis-related proteins, their activities, and comparative analysis of PR-1 type proteins. *Physiological and Molecular Plant Pathology*, *55*, 85–97.

Van Loon, L. C., Rep, M., & Pieterse, C. (2006). Significance of inducible defense-related proteins in infected plants. *Annual Review of Phytopathology*, *44*, 135–162.

Venturas, M., López, R., Martín, J., Gascó, A., & Gil, L. (2014). Heritability of *Ulmus minor* resistance to Dutch elm disease and its relationship to vessel size, but not to xylem vulnerability to drought. *Plant Pathology*, *63*, 500–509.

Vlot, A. C., Dempsey, D. M. A., & Klessig, D. F. (2009). Salicylic acid, a multifaceted hormone to combat disease. *Annual Review of Phytopathology*, *47*, 177–206.

Wang, D., Pajerowska-Mukhtar, K., Culler, A. H., & Dong, X. (2007). Salicylic acid inhibits pathogen growth in plants through repression of the auxin signaling pathway. *Current Biology*, *17*, 1784–1790.

Wang, H., Jiang, C., Wang, C., Yang, Y., Yang, L., Gao, X., & Zhang, H. (2015). Antisense expression of the fasciclin-like arabinogalactan protein *FLA6* gene in *Populus* inhibits expression of its homologous genes and alters stem biomechanics and cell wall composition in transgenic trees. *Journal of Experimental Botany*, *66*, 1291–1302.

Yadeta, K., & Thomma, B. (2013). The xylem as battleground for plant hosts and vascular wilt pathogens. *Frontiers in Plant Science*, *4*, 97.

SUPPORTING INFORMATION

Additional Supporting Information may be found online in the supporting information tab for this article.

How to cite this article: Perdiguero P, Sobrino-Plata J, Venturas M, Martín JA, Gil L, Collada C. Gene expression trade-offs between defence and growth in English elm induced by *Ophiostoma novo-ulmi*. *Plant Cell Environ*. 2018;41:198–214. https://doi.org/10.1111/pce.13085